




Article

Phylogeny and Biogeography of *Morus* (Moraceae)

Chen-Xuan Yang^{1,2,3}, Shui-Yin Liu^{2,3}, Nyree J. C. Zerega^{4,5} , Gregory W. Stull^{2,6}, Elliot M. Gardner^{7,8,9}, Qin Tian^{2,3}, Wei Gu^{2,3} , Qing Lu^{2,3}, Ryan A. Folk^{10,11}, Heather R. Kates¹⁰, Robert P. Guralnick¹⁰ , Douglas E. Soltis^{10,12}, Pamela S. Soltis¹⁰, Yue-Hua Wang¹ and Ting-Shuang Yi^{2,3,6,*}

- ¹ School of Life Sciences, Yunnan University, Kunming 650500, China; yangchenxuan@mail.kib.ac.cn (C.-X.Y.); wangyh58212@126.com (Y.-H.W.)
- ² Germplasm Bank of Wild Species, Yunnan Key Laboratory of Crop Wild Relatives Omics, Kunming Institute of Botany, Chinese Academy of Sciences, Kunming 650201, China; liushuiyin@mail.kib.ac.cn (S.-Y.L.); gwstull@gmail.com (G.W.S.); tianqin@mail.kib.ac.cn (Q.T.); guwei1@mail.kib.ac.cn (W.G.); luqing@mail.kib.ac.cn (Q.L.)
- ³ University of Chinese Academy of Sciences, Beijing 100049, China
- ⁴ Negaunee Institute for Plant Conservation and Action, Chicago Botanic Garden, Glencoe, IL 60022, USA; n-zerega@northwestern.edu
- ⁵ Plant Biology and Conservation Program, Northwestern University, Evanston, IL 60208, USA
- ⁶ CAS Key Laboratory for Plant Diversity and Biogeography of East Asia, Kunming Institute of Botany, Chinese Academy of Sciences, Kunming 650201, China
- ⁷ International Center for Tropical Botany, Institute of Environment, Florida International University, Miami, FL 33199, USA; elliot.gardner@gmail.com
- ⁸ National Tropical Botanical Garden, Kalāheo, HI 96741, USA
- ⁹ Department of Biology, Case Western Reserve University, Cleveland, OH 44106, USA
- ¹⁰ Florida Museum of Natural History, University of Florida, Gainesville, FL 32611, USA; rfolk@biology.msstate.edu (R.A.F.); hkates@ufl.edu (H.R.K.); robgur@gmail.com (R.P.G.); dsoltis@ufl.edu (D.E.S.); psoltis@flmnh.ufl.edu (P.S.S.)
- ¹¹ Department of Biological Sciences, Mississippi State University, Starkville, MS 39762, USA
- ¹² Department of Biology, University of Florida, Gainesville, FL 32611, USA
- * Correspondence: tingshuangyi@mail.kib.ac.cn



Citation: Yang, C.-X.; Liu, S.-Y.; Zerega, N.J.C.; Stull, G.W.; Gardner, E.M.; Tian, Q.; Gu, W.; Lu, Q.; Folk, R.A.; Kates, H.R.; et al. Phylogeny and Biogeography of *Morus* (Moraceae). *Agronomy* **2023**, *13*, 2021. <https://doi.org/10.3390/agronomy13082021>

Academic Editor: Teresa Navarro

Received: 8 July 2023
Revised: 28 July 2023
Accepted: 29 July 2023
Published: 30 July 2023



Copyright: © 2023 by the authors. Licensee MDPI, Basel, Switzerland. This article is an open access article distributed under the terms and conditions of the Creative Commons Attribution (CC BY) license (<https://creativecommons.org/licenses/by/4.0/>).

Abstract: The mulberry genus, *Morus* L. (Moraceae), has long been taxonomically difficult, and its species circumscription has only been defined recently. This genus comprises ca. 16 species distributed across Asia and the Americas, yet its biogeographic history remains poorly understood. In this study, we reconstructed the phylogeny and explored the biogeographic history of *Morus* using a combination of newly generated and previously published Hyb-Seq data. Our nuclear phylogeny recovered three well-supported geographic clades of *Morus* and showed that *M. notabilis* (China) is sister to the American clade plus the Asian clade. Multiple reticulation events among species of *Morus* and extensive incomplete lineage sorting (ILS) likely explain the difficulties in inferring phylogenetic relationships within the genus. Divergence time estimation indicated that *Morus* originated at the Eocene–Oligocene boundary, and current lineages started to diverge during the early Miocene, there is ambiguity surrounding the ancestral area with the two most likely regions being Sino-Himalaya or the Americas. Biogeographic inference and the fossil record suggest that *Morus* might have experienced extensive local extinction events during the Tertiary. *Morus* has expanded its distributional range through two dispersals from the Sino-Himalayan and Sino-Japanese regions to Southeast Asia. In summary, our new phylogenetic scheme and the biogeographic history presented here provide an essential foundation for understanding species relationships and the evolutionary history of *Morus*.

Keywords: ancestral area reconstruction; biogeography; dispersal; divergence times; *Morus*; phylogeny

1. Introduction

Mulberries (*Morus* L., Moraceae) are widely known and have great economic value in that the leaves of several species are the primary food source for silkworms (*Bombyx mori*

L.). Additionally, members of this genus provide edible fruits, fibers, medicine, and raw material for papermaking [1]. Species of *Morus* exhibit considerable morphological diversity (Figure 1; Table S1). More specifically, the breeding systems of *Morus* are monoecious or dioecious and the length of styles and syncarps (fruits) vary among species. These three characteristics are critical for species classification of *Morus* [1–4]. However, the evolution of these traits has not been extensively addressed and the value of these characters in *Morus* classification are largely unknown.



Figure 1. Images of leaves, infructescences, and male inflorescences of *Morus*. (A–C) *M. alba* L.; (D–F) *M. australis* Poir.; (G,H) *M. cathayana* Hemsl.; (I–K) *M. macroura* Miq.; (L–N) *M. mongolica* (Bur.) C.K.Schneid.; (O) *M. notabilis* C.K.Schneid.; (P,Q) *M. wittiorum* Hand.-Mazz.; (R,S) *M. serrata* Roxb. (S, immature infructescences); (T) *M. australis* var. *inusitata* (Lévl.) C.Y.Wu; (U) *M. rubra* L.; (V) *M. alba* (*M. mongolica* (Mor 55-951) from Gardner et al. [5]). Photographer: (A–F,I,J,L) by Che-Xuan Yang; (G,H,M) by Xin-Xin Zhu; (K,N,P,Q) by Qin-Wen Lin; (O) by Si-Yu Zhang; (R,S) by Jie Cai; (T) by Qin Tian (SFU); and (U,V) by Elliot M. Gardner.

Since Linnaeus [6] first established the genus *Morus* and described seven species, the circumscription and taxonomy of the genus have been challenging. Over the last 200-plus years, the number of recognized species, varieties, and subvarieties has proliferated. For example, Bureau [7] recognized six species, 20 varieties (16 under *M. alba* L.), and 12 subvarieties (11 under *M. alba*). Koidzumi [2] elevated many of these varieties to species and reduced others to synonymy, resulting in 24 species that were divided into two sections based on the length of the style: sect. *Macromorus* Koidz. (=sect. *Morus*) and sect. *Dolichostylae* Koidz. Leroy [8] classified 18 *Morus* species into three subgenera: subg. *Eumorus* J.F.Leroy (= subg. *Morus*) distributed in Asia and North America; subg. *Gomphomorus* J.F.Leroy distributed in South America; and subg. *Afromorus* A.Chevalier distributed in tropical Africa. Subsequently, Hotta [9] recognized 35 *Morus* species, and Chang et al. [3] recognized 16 *Morus* species, 11 of which are distributed in China.

Some of the explanations for species circumscription in *Morus* has been difficult include variable and continuous morphological traits, the recent global expansions of several species due to human transportation, and widespread interspecific hybridization facilitated by their wind-pollination breeding system and sympatry in several species [10–12].

Nepal and Purinton [4] and Nepal and Ferguson [13] reconstructed the phylogeny of *Morus* based on ITS and *trnL-trnF* sequences and found that the African *M. mesozygia* Stapf and the South American *M. insignis* Bureau formed a clade separate from the other species of *Morus*. A phylogenetic study by Gardner et al. [5] on the entire tribe Moreae using 686 loci recovered a monophyletic *Morus* s.s. and transferred *M. mesozygia* to *Afromorus mesozygia* (Stapf.) E.M.Gardner and *M. insignis* to *Paratrophis insignis* (Bureau) E.M.Gardner. This study recognized 16 *Morus* species but suggested that further work was needed to better understand species circumscription within the genus.

Most *Morus* species are distributed in temperate forests or mid-elevation tropical forests and are adapted to cooler climates, in contrast to most other members of Moraceae, which are largely distributed in subtropical and tropical regions (exceptions include *Broussonetia* L'Hér. ex Vent. and some *Maclura* Nutt.). The disjunct distribution of *Morus* in the Northern Hemisphere (ca. 13 Asian and 3 American species) makes the genus interesting biogeographically. Most of the Asian species are found in East and Southeast Asia, while western Asia has an endemic species, *M. nigra* L.

The disjunct distribution between eastern Asia and eastern North America is a major biogeographic pattern in the Northern Hemisphere and has been studied in many taxa (e.g., Xiang et al. [14]; Wen [15]; Jin et al. [16]; Gaynor et al. [17]). This disjunction is considered to comprise the remnants of once-widely distributed temperate forests during the Tertiary [15,18]. Tribe Artocarpeae (Moraceae) also has an Asian and American disjunction, and biogeographic reconstruction indicates that Artocarpeae likely originated in the Americas, and the Asian clade (*Artocarpus* J.R.Forst. and G.Forst.) split from the American clade (*Batocarpus* H.Karst. and *Clarisia* Ruiz and Pav.) during the Paleocene (55.24–65.03 million years ago (Mya)), when the North Atlantic Land Bridge was available for migration [19]. Previous studies have estimated divergence times for *Morus*. Zerega et al. [20] inferred the crown age of *Morus* at 23.3–43.3 Mya; however, only two species of *Morus* were included in the study (*M. alba* and *M. nigra*), and the phylogeny was based on just two loci. Subsequently, Gardner et al. [5] examined a much larger dataset (with 10 *Morus* species and 686 genes) and suggested that the genus originated during the Eocene. However, the biogeography of the entire genus has not been investigated. *Morus* is therefore a good taxon for examining the origins of disjunct distributions in the Northern Hemisphere.

We use a combination of published [5] and newly generated sequence data representing 686 and 100 nuclear loci from 11 of the 16 recognized *Morus* species, to resolve phylogenetic relationships and infer the biogeographic history of this genus. In addition, we reconstruct ancestral states of characters that have been historically used to differentiate species: style length, syncarp length, and breeding system. Our study provides a foundation for further evolutionary investigations and ultimately a taxonomic revision of *Morus*.

2. Materials and Methods

2.1. Taxon Sampling

The final dataset contained 17 samples of *Morus*, consisting of eight newly sequenced samples from the current study and nine samples from Gardner et al. [5] (Table 1). Four additional *Morus* samples used in Gardner et al. [5] were not included in this study after they were determined to be *M. alba* based upon a reexamination of the specimens (see details in Section 4.1). Seventeen samples were included in analyses representing 11 of 16 *Morus* species recognized by Gardner et al. [5], with *M. wittiorum* Hand.-Mazz being sampled for the first time in a molecular phylogenetic analysis. Each sampled species was represented by one or two individuals. Our sampling covered nearly the entire geographical distribution of the genus, including Asia and the Americas, but we were unable to sample *M. nigra*, whose native distributions is in Iran. Four other unsampled species (*M. boninensis* Koidz., *M. liboensis* S.S.Chang, *M. koordersiana* J.-F.Leroy, and *M. trilobata* (S.S.Chang) Z.Y.Cao) are endemic species to certain east Asian regions and would likely not affect our phylogenetic and biogeographic inferences.

The outgroup included 11 newly sequenced samples and 11 samples from Gardner et al. [5], representing a total of 12 species from 10 other genera of Moraceae (Table 1): 1 species each from *Trophis* P.Browne, *Afromorus* E.M.Gardner, *Paratrophis* Blume, *Taxotrophis* Blume, *Batocarpus*, *Maclura*, *Parartocarpus* Baill., and *Olmedia* Ruiz and Pav., and two species each from *Artocarpus* and *Ficus* L. Each outgroup species was represented by two individuals except for two species of *Ficus*.

2.2. DNA Extraction, Library Preparation, and Sequencing

Total genomic DNA of the new samples was extracted from leaf fragments taken from herbarium specimens (Table 1) using a CTAB protocol [21]. Sample quantification, library preparation, hybridization, and sequencing (150-bp paired-end reads) were conducted by RAPiD Genomics (Gainesville, FL, USA). For Hyb-Seq of 19 new samples, we used a set of 100 low-copy nuclear genes (hereafter, HybSeq100) that were designed for the phylogenomic analyses of the nitrogen-fixing clade (including Moraceae) and discussed in detail by Folk et al. [22], Kates et al. [23], Fu et al. [24], and Liu et al. [25].

2.3. Sequence Assembly and Dataset Processing

For the newly generated data, we removed adapters and low-quality bases of raw reads using Trimmomatic [26] with the parameters fa:2:30:10:8:TRUE. Cleaned reads were assembled using HybPiper v1.3.1 [27] using 100 protein sequences (corresponding to the 100 targeted genes) of *Arabidopsis thaliana* (L.) Heynh. as references. Exon contigs extracted from assemblies were aligned for each locus using MAFFT v7.305b [28]. We used the pipeline of KewHybSeqWorkshop [29] to remove the samples with long branches in each gene using ETE3 [30] with the parameters of inlen = 0.50, outlen = 0.90, and leaflen = 0.40. Columns with more than 50% gaps in each alignment were removed using trimAl [31].

To incorporate the sequence data of Gardner et al. [5] that were generated based on two probe sets, the Moraceae333 loci [27,32] and the Angiosperms353 loci [33], we assembled the HybSeq100 loci from the Hyb-Seq data of Gardner et al. [5] and recovered data for 43 genes. We also assembled the Moraceae333 and Angiosperms353 loci from the new Hyb-Seq data of this study and recovered 159 genes. We removed 45 loci for which data were obtained for fewer than three *Morus* samples or overlapped among three probe sets and generated a dataset of 157 nuclear genes shared among all 39 samples (17 *Morus* + 22 outgroup samples; hereafter, C157). For subsequent conflict and biogeographic analyses, a simplified C157 dataset was built by retaining one individual per species with the least missing data. In addition, a comprehensive dataset of 430 nuclear genes (hereafter, C430) was generated by combining the 157 genes from the C157 dataset, 51 genes only represented by newly sequenced samples, and 222 genes only represented by the samples of Gardner et al. [5].

Table 1. Taxon sampling information in this study.

Species	Collector and Number	Locality	Herbarium	Recovered Gene Number (Moraceae333/Angiosperms353/HybSeq100)	Accession Numbers	Tribe	Style Length	Syncarp Length	Breeding System
<i>Afromorus mesozygia</i> (Stapf) E.M.Gardner	ATBP 639	Uganda	MO	(1/4/81)	SAMN35653736 (new)	Moreae			
<i>Afromorus mesozygia</i> (Stapf) E.M.Gardner	Buckner 309	Central African	MO	(327/15/18)	SRR12282928	Moreae			
<i>Artocarpus altilis</i> (Parkinson) Fosberg	Lawrence J. Eilers 652	Honduras	OS	(NA/8/85)	SAMN35653737 (new)	Artocarpeae			
<i>Artocarpus altilis</i> (Parkinson) Fosberg	Breadfruit Institute grid no. K7	USA	PTBG	(319/NA/5)	SRR12282879	Artocarpeae			
<i>Artocarpus papuanus</i> (Becc.) Renner	E. F. de Vogel 3777	Indonesia	MO	(1/5/79)	SAMN35653738 (new)	Artocarpeae			
<i>Artocarpus papuanus</i> (Becc.) Renner	Zerega et al. 61	Papua New Guinea	NY	(314/NA/5)	SRR12283061	Artocarpeae			
<i>Batocarpus amazonicus</i> (Ducke) Fosberg	Nee 47112	NA	TEX	(2/20/84)	SAMN35653739 (new)	Artocarpeae			
<i>Batocarpus amazonicus</i> (Ducke) Fosberg	Berg et al. 18524	Brazil	K (K000946661)	(22/36/6)	ERS4414214	Artocarpeae			
<i>Ficus piresiana</i> Vázq.Avila and C.C. Berg	H. Medeiros 1587	Brasil	NY	(2/6/84)	SAMN35653740 (new)	Ficeae			
<i>Ficus sagittifolia</i> Warb. ex Mildbr. and Burret	Chase 19852		K	36/35/14)	ERS4414205	Ficeae			
<i>Maclura tricuspidata</i> Carrière	Pozorski 9826V03	NA	KUN	(NA/5/84)	SAMN35653741 (new)	Chlorophoreae			
<i>Maclura tricuspidata</i> Carrière	Gardner MOR 68-7917	USA	MOR	(287/8/15)	SRR12282950	Chlorophoreae			
<i>Morus alba</i> L.	A. C. Sanders 13809	USA	CAS	(NA/5/83)	SAMN35653742 (new)	Moreae	short	short	dioecy
<i>Morus alba</i> L.	Gardner MOR 920-26*1	USA	MOR	(321/7/12)	SRR12282946	Moreae	short	short	dioecy
<i>Morus australis</i> Poir.	M. Ono and S. Kobayashi	Japan	OS	(NA/5/86)	SAMN35653743 (new)	Moreae	long	short	dioecy
<i>Morus australis</i> Poir.	Gardner MOR 241-71*6	USA	MOR	(322/8/14)	SRR12282942	Moreae	long	short	dioecy

Table 1. Cont.

Species	Collector and Number	Locality	Herbarium	Recovered Gene Number (Moraceae333/Angiosperms353/HybSeq100)	Accession Numbers	Tribe	Style Length	Syncarp Length	Breeding System
<i>Morus cathayana</i> Hemsl.	Gaoligong Shan Biodiversity Survey 19616	China	CAS	(0/6/80)	SAMN35653744 (new)	Moreae	short	short	monoecy
<i>Morus cathayana</i> Hemsl.	Wilson 10	China	F	(96/1/1)	SRR12282938	Moreae	short	short	monoecy
<i>Morus celtidifolia</i> Kunth	Juan Calzada 20974	Mexico	TEX	(2/13/84)	SAMN35653745 (new)	Moreae	short	short	dioecy vs. monoecy
<i>Morus celtidifolia</i> Kunth	Sandoval and Gutierrez 637	Mexico	MO	(332/19/19)	SRR12282937	Moreae	short	short	dioecy vs. monoecy
<i>Morus macroura</i> Miq.	Gardner 28	USA	CHIC	(329/13/18)	SRR12282930	Moreae	short	long	dioecy
<i>Morus microphylla</i> Buckley	Fishbein et al. 1058	Mexico	F	(325/17/19)	SRR12282927	Moreae	short	short	dioecy
<i>Morus mongolica</i> (Bur.) C.K.Schned.	Liu Xin-Yuan 5257	China	CAS	(1/5/72)	SAMN35653746 (new)	Moreae	long	short	dioecy
<i>Morus notabilis</i> C.K.Schneid.	Gaoligong Shan Biodiversity Survey 29353	China	CAS	(1/6/83)	SAMN35653747 (new)	Moreae	long	long	dioecy
<i>Morus notabilis</i> C.K.Schneid.	NA	China	NA	(331/34/84)	SRR8138828	Moreae	long	long	dioecy
<i>Morus rubra</i> L.	Steven R. Hill 36694	USA	CAS	(NA/5/84)	SAMN35653748 (new)	Moreae	short	short	dioecy
<i>Morus rubra</i> L.	Gardner 141	USA	CHIC	(326/9/12)	SRR12282922	Moreae	short	short	dioecy
<i>Morus serrata</i> Roxb.	Koelz 4788	India	F	(269/5/9)	SRR12282920	Moreae	short	short	dioecy
<i>Morus wittiorum</i> Hand.-Mazz.	Zhang Wei	China	KUN	(1/5/85)	SAMN35653749 (new)	Moreae	short	long	dioecy
<i>Olmedia aspera</i> Ruiz and Pav.	J. A. Duke 13250(3)	Panama	OS	(NA/4/78)	SAMN35653750 (new)	Olmedieae			
<i>Olmedia aspera</i> Ruiz and Pav.	Fuentes et al. 5323	Bolivia	MO	(244/3/7)	SRR12282905	Olmedieae			
<i>Parartocarpus venenosus</i> (Zoll. ex Moritzi) Becc.	T. J. Motley et al. 21	Papua New Guinea	NY	(NA/4/67)	SAMN35653751 (new)	Parartocarpeae			
<i>Parartocarpus venenosus</i> (Zoll. ex Moritzi) Becc.	Zerega et al. 874	Malaysia	F, SAN	(207/0/5)	SRR3907334	Parartocarpeae			

Table 1. Cont.

Species	Collector and Number	Locality	Herbarium	Recovered Gene Number (Moraceae333/Angiosperms353/HybSeq100)	Accession Numbers	Tribe	Style Length	Syncarp Length	Breeding System
<i>Paratrophis insignis</i> (Bureau) E.M.Gardner	D. E. Breedlove 31069	Mexico	CAS	(1/3/83)	SAMN35653752 (new)	Moreae			
<i>Paratrophis insignis</i> (Bureau) E.M.Gardner	Vasquez and Francis 28068	Peru	F	(332/18/18)	SRR12282932	Moreae			
<i>Taxotrophis macrophylla</i> (Blume) Boerl.	D. D. Soejarto et al. 10673	Vietnam	NY	(0/4/81)	SAMN35653753 (new)	Moreae	short	short	dioecy
<i>Taxotrophis macrophylla</i> (Blume) Boerl.	Soejarto et al. 10673	Vietnam	F	(323/NA/19)	SRR12282865	Moreae	short	short	dioecy
<i>Trophis mexicana</i> (Liebm.) Bureau	Rafael García S. 539	Mexico	TEX	(6/16/87)	SAMN35653754 (new)	Moreae			
<i>Trophis mexicana</i> (Liebm.) Bureau	Stevens and Montiel 27939	Nicaragua	MO	(322/4/14)	SRR12282883	Moreae			

Note: "NA" represents the missing information; "new" indicates the new generated sequences.

2.4. Phylogenetic Analysis

We conducted maximum likelihood analyses on three concatenated matrices (C157, simplified C157, and C430) using RAxML v8.2.11 [34] with the GTRGAMMA model and 200 bootstrap replicates. Individual ML gene trees for the three datasets were reconstructed with the same parameters as above using RAxML. A species tree for each dataset was then inferred by ASTRAL v5.6.3 [35] using gene trees, with support values measured using local posterior probabilities (LPP).

2.5. Topologies Tests

To compare alternative topologies, we carried out the approximately unbiased (AU) test [36] based on the simplified C157 dataset. The log-likelihood value per site was calculated using RAxML with the GTRGAMMA model. The implementation of the AU test and calculation of p -values were performed using CONSEL v1.6 [37]. We also performed a polytomy test [38] to evaluate whether a given branch in the ASTRAL tree could reject the null hypothesis using the option “-t 10” of ASTRAL based on the simplified C157 dataset. If the null hypothesis cannot be rejected ($p > 0.05$), the bifurcating topology can be replaced by a polytomy [38].

2.6. Coalescent Simulations and Network Analyses

To explore the causes of discordance among phylogenetic trees, we first used coalescent simulations to examine whether ILS alone is sufficient to explain the observed discordance based on the C157 dataset, following Garcia et al. [39] and Wang et al. [40]. We simulated 1000 trees under the coalescent using the script generateCoalescentTrees.py [41] and mapped these simulated trees on the ASTRAL tree and the concatenated ML tree inferred from the C157 dataset using PhyParts [42] and the script phypartspiecharts.py (<https://github.com/mossmatters/MJPythonNotebooks/blob/master/phypartspiecharts.py>, accessed on 1 September 2022). In addition, we inferred phylogenetic networks using the “InferNetwork_MPL” command in PhyloNet v3.8.2 [43] and allowed a maximum number of reticulations from 0 to 5 and 10 runs for each search. The gene trees from the simplified C157 dataset (with branches of bootstrap support (BS) < 50% collapsed) were utilized for network analysis. To reduce the computational burden, we only included the closest outgroup, *T. mexicana*. We calculated the Akaike Information Criterion (AIC) values for the six networks to choose the optimal model. The number of parameters for AIC calculation was set to the number of estimated branch lengths and inheritance probabilities (γ). The proportion of genetic contributions of parental populations at a given reticulated node was indicated by the inheritance probabilities (γ). The log-likelihood scores of bifurcating trees were calculated using the command “CalGTProb” [44].

2.7. Divergence Time Estimation

We used one secondary and three fossil calibrations for divergence-time estimation following Zhang et al. [45]: (1) one secondary calibration to constrain the crown age of Moraceae with a minimum age of 73.2 Mya and a maximum age of 84.7 Mya; (2) a wood fossil of *Artocarpoxylon deccanensis* Mehrotra, Prakash, and Bande from the early Tertiary [46] to constrain the minimum stem age of *Artocarpus* to 64 Mya; (3) an achene fossil of *Ficus lucidus* Chandler from the Paleocene-Eocene boundary [47] to constrain the minimum stem age of *Ficus* to 56 Mya; and (4) an achene fossil of *M. tymensis* Dorofeev from the Eocene–Oligocene boundary [48] to constrain the minimum stem age of *Morus* to 33.9 Mya.

The divergence times were estimated in treePL v1.0 [49,50] using the best concatenated ML tree from the simplified C157 dataset, with a smoothing parameter of 0.0001 that was determined by cross-validation tests. Following the method of Maurin [50], we also generated 1000 bootstrap trees using RAxML with the topology fixed by the best concatenated ML tree from the simplified C157 dataset and its concatenated matrix as the input alignment. To estimate uncertainty in divergence times, treePL analyses were

conducted across 1000 bootstrap trees. We used TreeAnnotator v2.6.7 [51] to summarize the 1000 bootstrap dated trees into a consensus tree, including 95% confidence intervals (CI) for each node. The configuration files of all treePL analyses are provided in the Dryad Digital Repository (<https://doi.org/10.5061/dryad.bzkh189g1>, accessed on 8 June 2023).

2.8. Ancestral Area Reconstruction

We compiled the distribution information for each *Morus* species based on Zhou and Gilbert [1], Wunderlin [52], and Plants of the World Online (<https://powo.science.kew.org/>, accessed on 1 September 2022). Given the extant distribution of *Morus* and the floristic delineations proposed for Asia [53,54], we delimited four biogeographic regions: (A) Sino-Japan, including most of China, Mongolia, Japan, and Korea; (B) Sino-Himalaya, including the Hengduan Mountains and the Qinghai–Tibet Plateau (i.e., Yunnan, Tibet, and western Sichuan) of China, Bhutan, Nepal, and the Himalayan area of India; (C) Southeast Asia, including Southeast China (i.e., Guangdong, Hainan, and Taiwan), India, Indonesia, Malaysia, Myanmar, Sikkim, and Thailand; and (D) the Americas.

Ancestral area reconstruction was conducted using BioGeoBEARS [55] with unconstrained dispersal routes. The consensus dated tree from the simplified C157 dataset from treePL was used for biogeographic analysis. We tested three biogeographic models (i.e., DEC, DIVALIKE, and BAYAREA) provided by BioGeoBEARS and selected the best-fit model using the log-likelihood (LnL) and AIC values. The probabilities of ancestral range and the number and type of biogeographic events were estimated using the BSM implemented in BioGeoBEARS with 100 replicates under the best model inferred by the LnL and AIC values.

2.9. Ancestral Character State Reconstruction

To explore morphological evolution in *Morus*, we conducted ancestral reconstruction for three reproductive characters: breeding system, syncarp length, and style length. The morphological characters were collected from Zhou and Gilbert [1], Wunderlin [52], and Berg [56] (Table 1; Table S1). Following Zhou and Gilbert [1] and Koidzumi [2], we scored (1) the breeding system as either monoecy, dioecy, or dioecy and monoecy; (2) the syncarp length as short (equal and less than 2.5 cm) or long (more than 2.5 cm); and (3) the style length as short (equal and less than 2 mm) or long (more than 2 mm). The consensus dated tree from the simplified C157 dataset from treePL was used for ancestral state reconstruction but was pruned to retain only the sister group of *Morus*, *T. mexicana*. Ancestral character states were estimated using the continuous-time Markov chain (Mk) model in phytools v1.0-3 [57].

3. Results

3.1. Characteristics of Datasets and Monophyly of Sampled Species

The two datasets (C157 and C430) varied by gene coverage in each species, taxon coverage, and alignment length of each gene (Supplementary Table S2). In the C157 dataset, the number of recovered genes per species ranged from 25 (*B. amazonicus* (Berg et al., 18524)) to 157 (*M. notabilis* C.K.Schneid. (SRR8138828)); the alignment length of each gene ranged from 285 bp to 3159 bp; and the concatenated matrix had 205,046 bp. In the C430 dataset, the number of recovered genes per species ranged from 41 (*B. amazonicus* (Berg et al., 18524)) to 425 (*M. notabilis* (SRR8138828)); the alignment length of each gene ranged from 159 bp to 3969 bp; and the concatenated matrix comprised 512,346 bp.

Across the 23 sampled Moraceae species, 16 species (including six species of *Morus* (*M. alba*, *M. australis* Poir., *M. cathayana* Hemsl., *M. celtidifolia* Kunth, *M. notabilis*, and *M. rubra* L.) and ten outgroup species) were represented by two individuals; these species were each monophyletic except for three *Morus* species (*M. australis*, *M. cathayana*, and *M. celtidifolia*) that were not monophyletic in certain analyses. The two samples of *M. australis* were resolved as a sister pair with moderate support in the concatenated ML trees based on the C157 (BS = 80) and C430 matrices (BS = 68; Figures 2 and S2), but were resolved

as a grade in both ASTRAL trees (Figures 2 and S2). The two samples of *M. cathayana* formed a clade with moderate support (BS = 74) in the concatenated ML tree based on the C157 matrix. In contrast, they were resolved as a grade in the concatenated ML tree based on the C430 matrix and the ASTRAL trees of the two datasets (Figures 2 and S2). The two samples of *M. celtidifolia* did not form a clade in any of the four phylogenetic trees (Figures 2 and S2).

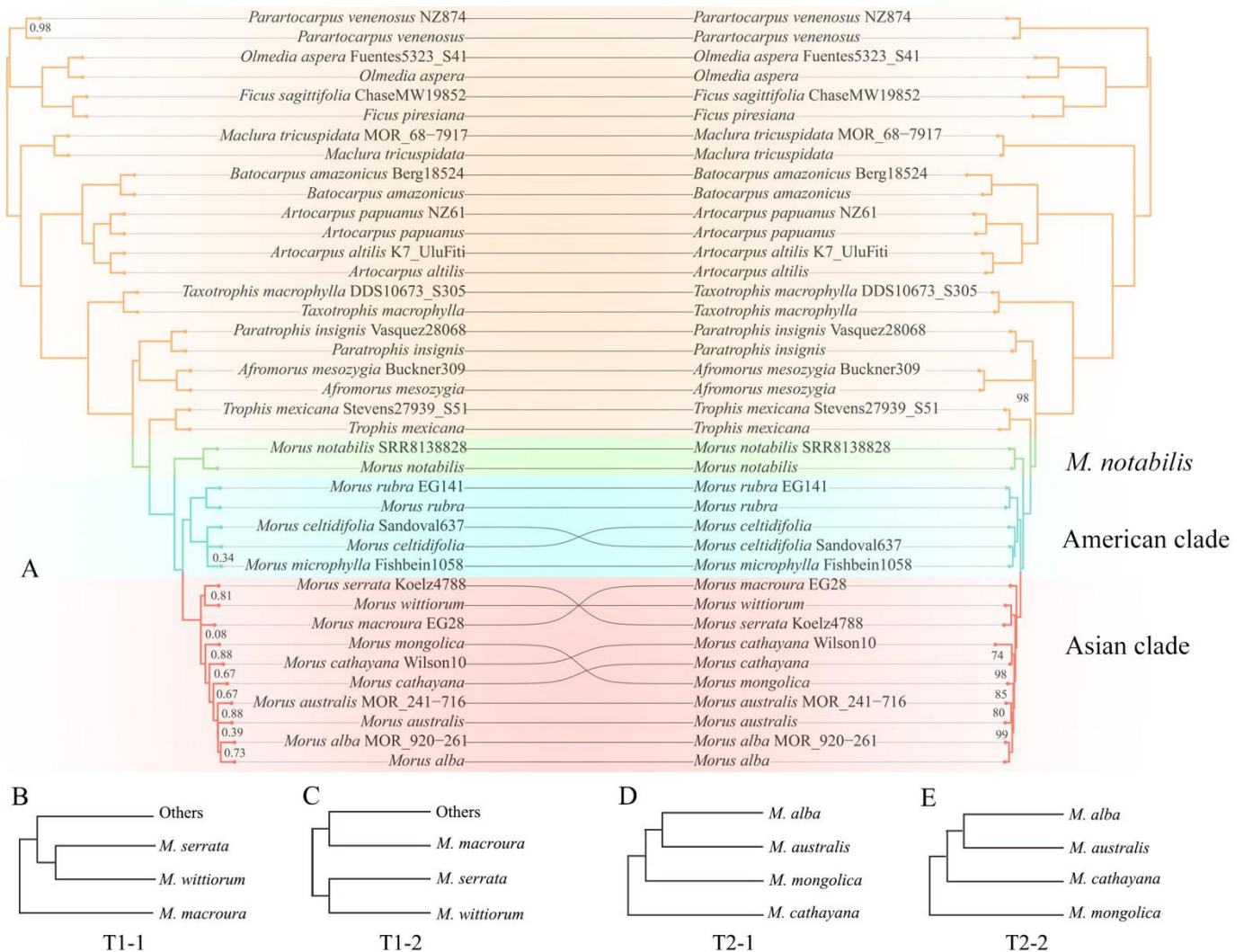


Figure 2. Phylogenetic trees showing concordant and conflicting relationships in *Morus*. (A) Comparison of the ASTRAL tree (left) and concatenated ML tree (right) of *Morus* based on the C157 matrix. All nodes have a support value of LPP = 1 (left) or BS = 100% (right) unless otherwise indicated. (B,C) Two alternative topologies for the earliest diverged lineages in the Asian clade of *Morus*. Topology T1-1 is from the concatenated ML tree in Figure 2A and the concatenated and ASTRAL trees in Supplementary Figure S2, while topology T1-2 is from the ASTRAL tree in Figure 2A. (D,E) Two alternative topologies for the branch connecting *M. mongolica* and *M. cathayana* toward the tips of the Asian clade of *Morus*. Topology T2-1 is from the concatenated ML tree in Figures 2A and S2, while topology T2-2 is from the ASTRAL tree in Figures 2A and S2.

3.2. Phylogenetic Relationships and Discordance

The concatenated and ASTRAL trees based on the two datasets were largely congruent except for several nodes near the tips (Figures 2A and S2). All phylogenetic trees showed a monophyletic *Morus* as defined by Gardner et al. [5] (BS = 100; LPP = 1), consisting of three major lineages: *M. notabilis* was fully supported as sister to the American clade + the

Asian clade (BS = 100, LPP = 1; Figures 2A and S2). The American clade with full support included three species, with the lineage of *M. celtidifolia* + *M. microphylla* Buckley sister to *M. rubra* (BS = 100, LPP = 1) in all phylogenetic trees of the two datasets.

The identity of the sister lineage to the rest of the Asian clade was a source of conflict among the different trees, involving three species, *M. macroura* Miq., *M. wittiorum*, and *M. serrata* Roxb. The concatenated ML trees based on the two datasets and the ASTRAL tree of the C430 dataset fully supported *M. macroura* as sister to the rest of the Asian clade (BS = 100, LPP = 1; T1-1, Figures 2B and S2). This topology was supported by the AU test ($p = 0.999$; Table S3). The ASTRAL tree based on the C157 dataset supported a lineage of *M. serrata* + *M. wittiorum* as sister to the rest of the Asian clade (LPP = 0.81; T1-2, Figures 2C and S2). However, that topology T1-2 was not supported by the AU test ($p < 0.05$; Table S3).

Moreover, the phylogenetic relationships among four additional species (*M. cathayana*, *M. mongolica* (Bur.) Schneid., *M. australis*, and *M. alba*) in the Asian clade were also a source of conflict among the different trees. The concatenated ML trees of the two datasets both revealed a well-supported topology of (*M. cathayana*, (*M. mongolica*, (*M. australis*, *M. alba*))) (BS = 97–98; T2-1, Figures 2D and S2), while the two ASTRAL trees both supported a topology of (*M. mongolica*, (*M. cathayana*, (*M. australis*, *M. alba*))) (LPP = 0.66–1; T2-2, Figures 2E and S2). The AU test failed to reject either of these two conflicting topologies (topology T2-1: $p = 0.72$; topology T2-2: $p = 0.28$; Table S3). The polytomy test for the branch connecting *M. mongolica* and *M. cathayana* failed to reject the null hypothesis ($p > 0.05$; Figure S3), indicating that this node can be replaced by a polytomy.

3.3. Coalescent Simulations and Phylogenetic Networks

We plotted the 1000 trees simulated under the coalescent against the ASTRAL tree based on the C157 dataset and found that all nodes within *Morus* were present in a set of simulated trees (76–889 trees; Figure 3), indicating all topologies were generally within ILS prediction. The observed discordances within the Asian clade of *Morus* can therefore be explained partly by ILS. For example, topologies T1-1 and T1-2 of *M. macroura*, *M. wittiorum*, and *M. serrata* were supported by 9.6% (Figure S4) and 7.6% (Figure 3) of the simulated trees, respectively. Topologies T2-1 and T2-2 of *M. cathayana*, *M. mongolica*, *M. australis*, and *M. alba* were supported by 2.6% (Figure S4) and 21.1% (Figure 3) of simulated trees, respectively.

The PhyloNet analyses indicated that *Morus* had a complex reticulate history (Figure 4). Three hybridization events were detected in the best network of *Morus* (Figure 4; Table 2). Specifically, the extant *M. notabilis* was inferred to have gene flow from the ancestor of the Asian clade with a genetic contribution of 0.349 (Figure 4). The ancestor of the clade of *M. serrata* + *M. cathayana* + *M. mongolica* + *M. alba* + *M. australis* was inferred to have gene flow from the ancestor of *M. notabilis* with a small inheritance probability ($\gamma = 0.0523$; Figure 4). The third hybridization event was detected within the Asian clade of *Morus*, where the extant *M. cathayana* had gene flow from the ancestor of *M. macroura* with an inheritance probability of 0.5 (Figure 4).

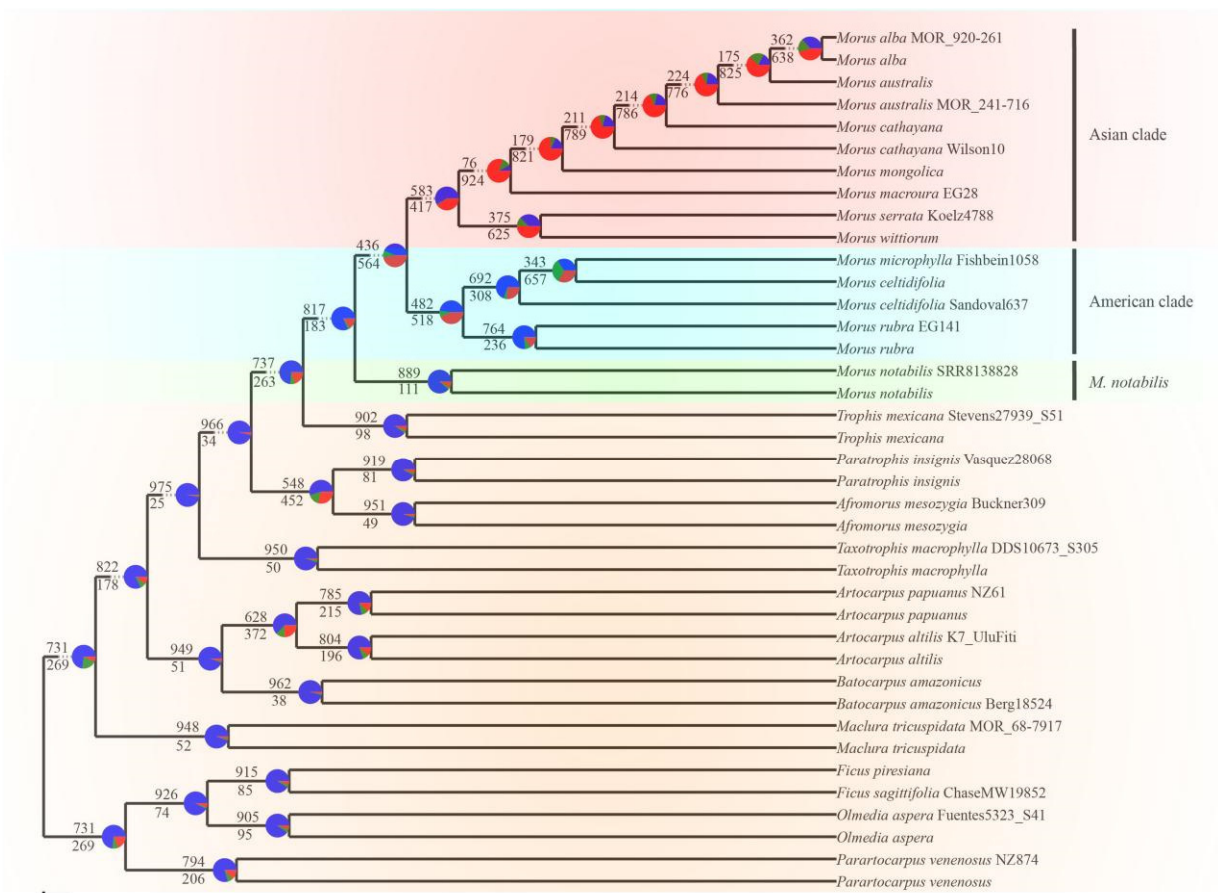


Figure 3. The result of coalescent simulations with 1000 trees simulated under the coalescent mapped against the ASTRAL tree of the simplified C157 dataset. The numbers near the branches indicate the number of simulated trees that are concordant (above) and discordant (below) with a given branch. The pie chart at each node indicates the proportion of simulated trees that are concordant (blue) with a given node, support a dominant alternative topology (green), and support the remaining alternative topologies (red).

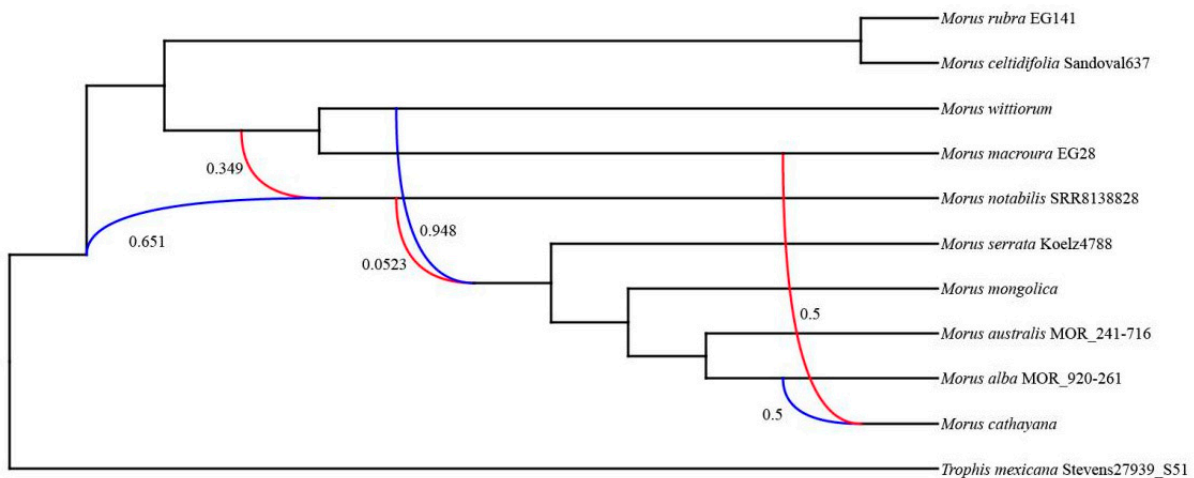


Figure 4. The optimal phylogenetic network of *Morus*. The values next to the curved lines indicate the inheritance probabilities (γ). The red line indicates the minor edge of a hybridization event (i.e., with a smaller γ), while the blue line indicates the major edge of a hybridization event (i.e., with a greater γ).

Table 2. Model selection among phylogenetic networks.

Topology	LnL	Parameters	Number of Hybridizations Event Allowed	Number of Hybridizations Event Detected	AIC	AICc	BIC
Network 0	−966.4673	19	0	0	1970.9346	1886.4902	1978.4947
Network 1	−948.2423	21	1	1	1938.4846	1854.4846	1946.8404
Network 2	−944.8661	23	2	2	1935.7322	1850.8091	1944.8838
Network 3	−910.9233	25	3	3	1871.8465	1785.1799	1881.7939
Network 4	−942.8554	27	4	4	1939.7109	1850.7697	1950.4541
Network 5	−909.6192	29	5	5	1877.2384	1785.6594	1888.7773
ASTRAL tree	−1205.3261	25	NA	NA	2460.6522	2373.9855	2470.5995
Concatenated ML tree	−1824.0011	25	NA	NA	3698.0022	3611.3355	3707.9496

Note: The optimal model is highlighted in bold.

3.4. Divergence Times

The result of divergence time estimation (Figure 5; Table 3) suggests the crown age of *Morus* is 18.94 Mya (95% CI: 15.17–23.07 Mya). *Morus notabilis* diverged from the remaining species of *Morus* at 18.94 Mya (95% CI: 15.17–23.07 Mya). The divergence time was 13.36 Mya (95% CI: 11.04–16.33 Mya) between the American clade and the Asian clade. The crown ages of the American clade and the Asian clade are 8.16 Mya (95% CI: 6.70–10.03 Mya) and 6.92 Mya (95% CI: 6.56–7.36 Mya), respectively.

Table 3. The estimated divergence times and ancestral area probabilities of major lineages in *Morus* based on the simplified C157 matrix.

Nodes	Age (Mya)	95% CI of Age (Mya)	Range Probabilities
SN of <i>Morus</i>	33.90 *	33.90–33.90 *	ABD: 0.203; BD: 0.167; BCD: 0.125
CN of <i>Morus</i>	18.94	15.17–23.07	BD: 0.253; ABD: 0.233; B: 0.144
SN of Asian + American clade in <i>Morus</i>	18.94	15.17–23.07	BD: 0.253; ABD: 0.233; B: 0.144
CN of Asian + American clade in <i>Morus</i>	13.36	11.04–16.33	ABD: 0.284; BD: 0.273; AB: 0.123
SN of Asian clade in <i>Morus</i>	13.36	11.04–16.33	ABD: 0.284; BD: 0.273; AB: 0.123
CN of Asian clade in <i>Morus</i>	6.92	6.56–7.36	AB: 0.728; B: 0.115
SN of American clade in <i>Morus</i>	13.36	11.04–16.33	ABD: 0.284; BD: 0.273; AB: 0.123
CN of American clade in <i>Morus</i>	8.16	6.70–10.03	D: 0.574; BD: 0.205; AD: 0.112
SN of Moreae	78.34	76.77–79.68	
CN of Moreae	56.68	54.20–58.98	
SN of <i>Trophis</i> + <i>Morus</i>	36.26	35.89–36.61	
SN of <i>Paratrophis</i> + <i>Afromorus</i>	36.26	35.89–36.61	
CN of <i>Paratrophis</i> + <i>Afromorus</i>	32.25	30.37–34.21	
SN of Maclueae + (Artocarpeae + Moreae)	84.67	84.63–84.69	
CN of Maclueae + (Artocarpeae + Moreae)	82.99	82.38–83.48	
SN of Artocarpeae + Moreae	82.99	82.38–83.48	
CN of Artocarpeae + Moreae	78.34	76.77–79.68	
SN of Artocarpeae	78.34	76.77–79.68	
CN of <i>Artocarpus</i>	42.97	37.69–48.01	
SN of Parartocarpeae + (Olmedieae + Ficeae)	84.67	84.63–84.69	
CN of Parartocarpeae + (Olmedieae + Ficeae)	80.02	78.81–81.11	
SN of Olmedieae + Ficeae	80.02	78.81–81.11	
CN of <i>Ficus</i>	25.02	21.76–28.27	

Note: "*" denotes the age of fossil calibration. Abbreviations: SN, Stem node; and CN, crown node.

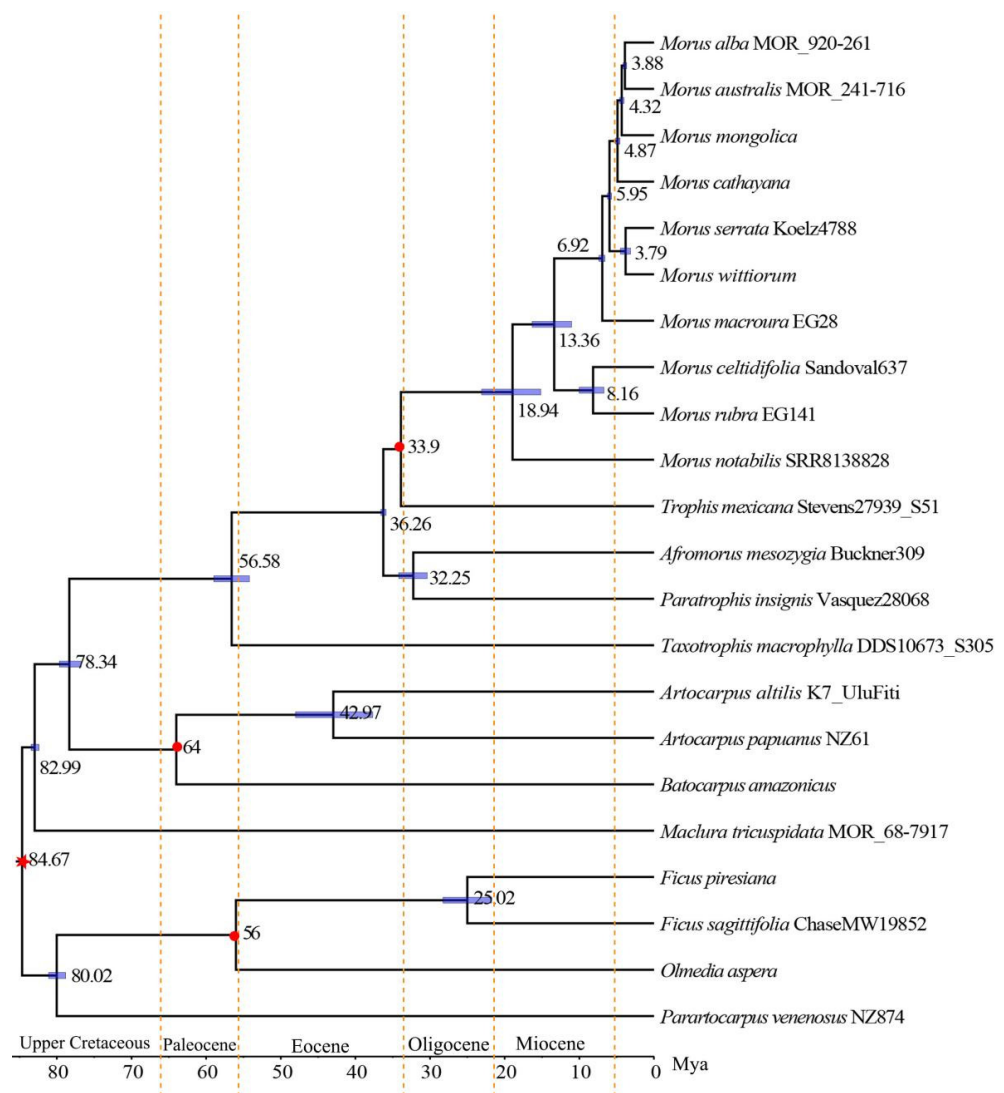


Figure 5. Time-calibrated tree of *Morus* estimated in treePL based on the simplified C157 dataset. The red dots indicate the positions of fossil calibrations. The red star indicates the position of secondary calibration. The value next to the node indicates the mean age summarized based on the 1000 dated bootstrap trees. The blue bar at each node indicates the 95% CI age summarized based on the 1000 dated bootstrap trees.

3.5. Ancestral Area Reconstruction

According to the LnL and AIC values (Table S4), the BAYAREALIKE model (LnL = -25.83 , AIC = 55.67) was the best-fit biogeographic model for the simplified C157 dataset (Figure 6). Under the BAYAREALIKE model, the most recent common ancestor (MRCA; i.e., crown node) of *Morus* was inferred to have originated in a widespread region comprising Sino-Himalaya and the Americas with a low probability (BD: 0.253, ABD: 0.233; Table 3). A local extinction event was inferred to have occurred in the lineage currently represented only by *M. notabilis*, sister to the rest of *Morus*, which is currently present only in the Sino-Himalaya region and absent from its ancestral area of the Americas during the early Miocene (Figure 6). An expanded range including Sino-Japan, Sino-Himalaya, and the Americas was reconstructed as the ancestral area for the MRCA of the American clade and the Asian clade (ABD: 0.284, BD: 0.273; Table 3). Following the divergence between the American clade and the Asian clade in the middle Miocene (Figure 6), local extinctions occurred in each of these two geographical clades. The MRCA of the American clade was most likely distributed within the Americas (D: 0.574, BD: 0.205; Table 3). While the Asian

clade was most likely distributed within a contracted region including the Sino-Japanese and Sino-Himalayan areas (AB: 0.728, B: 0.115; Table 3). Within the Asian clade, two dispersal events were found to have extended the distribution of *Morus* to a new region, Southeast Asia, during the late Miocene to the middle Pliocene. The BMS analysis showed that sympatric speciation was the dominant biogeographic events (60.57%) in shaping the diversification of *Morus*, followed by the anagenetic dispersal events (39.43%).

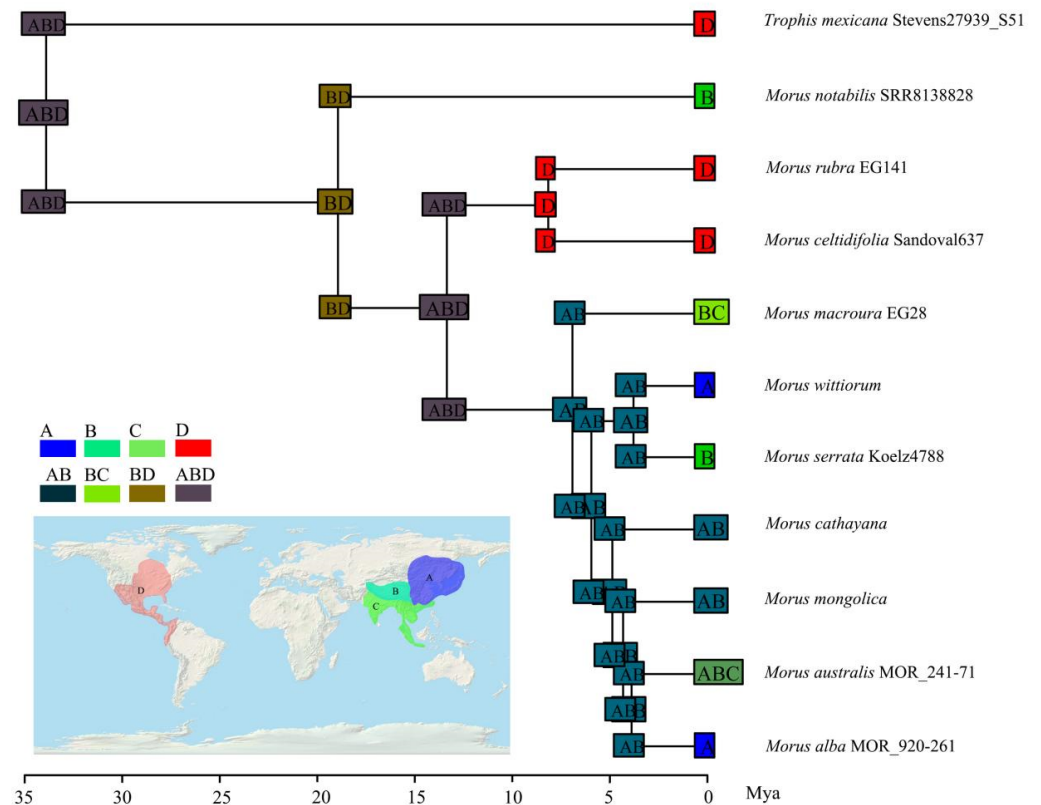


Figure 6. Ancestral area reconstruction of *Morus* under the BAYAREALIKE model in BioGeoBEARS based on the simplified C157 dataset. A, Sino-Japan; B, Sino-Himalaya; C, Southeast Asia; D, the Americas.

3.6. Ancestral Character State Reconstruction

The MRCA of *Morus* was inferred to be dioecious (Figure 7A), with a short syncarp (less than 2.5 cm; Figure 7B), and short or long style length (Figure 7C). We found that these reproductive characters (breeding system, syncarp length, and style length) have one or multiple transition across the phylogeny of *Morus*. The character states of monoecy and dioecy + monoecy both evolved from a single transition. The transition from dioecious to monoecy occurred in the branch leading to *M. cathayana*, while the transition from dioecious to dioecy + monoecy occurred in the branch leading to *M. celtidifolia*. A long syncarp was inferred as a derived state and evolved three times independently, once each in the branch leading to *M. notabilis*, *M. macroura*, and *M. wittiorum*. Due to the similar probabilities of long and short style, the ancestral state of style length is ambiguous for the MRCA of *Morus*, yet only three extant species (*M. australis*, *M. mongolica*, and *M. notabilis*) have a long style.

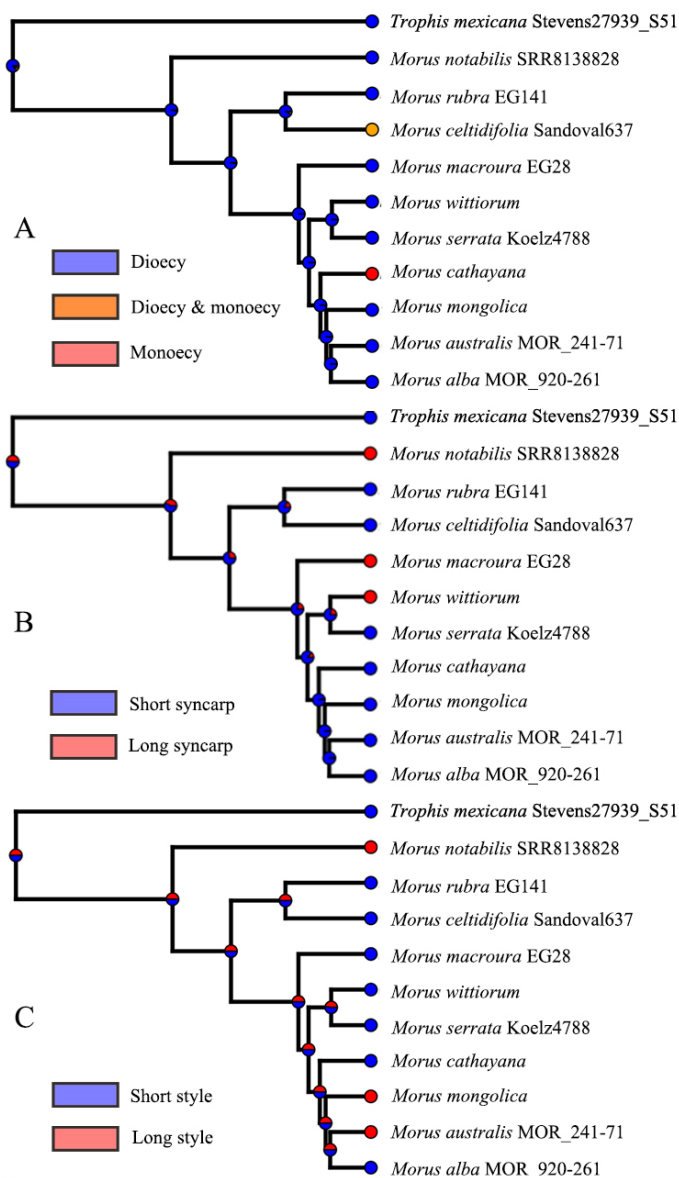


Figure 7. Ancestral state reconstructions for three reproductive traits of *Morus* under the Mk model. The pie charts at the nodes indicate the probabilities of ancestral states. Panels (A–C) show the results of ancestral reconstructions for breeding system, syncarp length, and style length of *Morus*, respectively.

4. Discussion

4.1. Further Clarification of Species Delimitation in *Morus*

Shifting species concepts and cryptic characters separating species can make identification of *Morus* specimens difficult. Determinations found on herbarium specimens must therefore be treated with caution. Upon re-examining the specimens sequenced by Gardner et al. [5], we found four of them to warrant re-determination. Specimens of *M. cathayana* (Nie, 92144; Figure S1E), *M. kagayamae* Koidz. (AA20187-A; Figure S1G), *M. mongolica* (Gardner, MOR 55-95*1; Figure 1V), and *M. nigra* (Gardner, 29; Figure S1K) were all re-identified as *M. alba*, although the characters of Gardner 29 are somewhat intermediate between *M. alba* and *M. nigra*. We note that the problem of misidentification extends particularly to living collections, as the latter two of these (Gardner, MOR 55-95*1 and Gardner, 29) came from trees cultivated in botanic gardens. Following these re-determinations, the sampling employed by Gardner et al. [5] did not contain any samples of *M. indica* L., *M. kagayamae*, or *M. mongolica*, and contained only one of *M. cathayana*.

While comprehensive species delimitation lies outside the scope of this study and the sampling employed here, our results, combined with morphological observations, nevertheless provide some insight into which species are likely distinct and which require further investigation with intensive sampling. Three species (*M. alba*, *M. notabilis*, and *M. rubra*) with two samples each were monophyletic in the current study (Figures 2A and S2), and two more, *M. macroura* and *M. serrata*, were monophyletic with at least two samples each in Gardner et al. [5]. These species all have unique identifying traits (Table S1) and appear to be distinct species. Two additional species (*M. australis* and *M. cathayana*) were monophyletic in certain analyses but not in others (also in Gardner et al. [5] for *M. australis*); while these species certainly warrant further investigation with more intensive sampling, their clear and consistent diagnostic characters support the suggestion that they are coherent species. *Morus microphylla* represented by two samples did not form a clade in Gardner et al. [5] because *M. celtidifolia* was nested within them. Meanwhile, two samples of *M. celtidifolia* in the current study did not form a clade because *M. microphylla* was nested within them. These two species (*M. celtidifolia* and *M. microphylla*) share similar morphological traits including leaf blades sometimes 3–5-lobed and female flowers with 0–0.2 mm styles (Figure S1; Table S1). We therefore follow Berg [56] in considering *M. microphylla* a synonym of *M. celtidifolia*. We note, however, that Nepal and Purinton [4] considered them distinct, separating them on the basis of leaf size, shape, and indumentum, habit, and infructescence size—differences no less substantial than those that separate some other species. Further study with increased sampling is therefore warranted for this complex.

Only one sample each of *M. mongolica*, *M. nigra*, and *M. wittiorum* was included in the current study or previous studies [4,13]. Nevertheless, on the basis of their unique identifying traits (Table 1), we consider them distinct species. The leaf margins of *M. mongolica* are serrated and have long or short spines on their teeth [1], making this species easy to distinguish from other *Morus* species. *Morus nigra* is native to western Iran and is now cultivated globally for its delicious and valuable fruits. The diagnostic feature of *M. nigra* is its abaxially pubescent leaf [1] (Table S1), and this species should also be a distinct species. In addition, *Morus wittiorum* can be identified by its leaf margin, which is either subentire or has teeth only at the apex [1].

Five species of *Morus* have not been sampled in any molecular phylogenetic study. *Morus boninensis* is an endemic species of the Bonin (Ogasawara) Islands, Japan, which is characterized by its long styles and glabrous leaf blades [58] (Table S1). *Morus liboensis* is an endemic species of Libo County, China, which is distinguished from *M. wittiorum* by its short styles and syncarps of 2.5–3.7 cm [59] (Table S1). *Morus trilobata* is an endemic species of Kaili County, China, and was first published as a variety of *M. australis* [59]. Cao [60] recognized it as a distinct species because it has entire leaf margins, long female inflorescences (2–4 cm), and short styles (Table S1), clearly distinguishing it from *M. australis*. These above three species should be distinct species based on their distinct morphological traits (Table S1).

Morus kagayamae was considered indistinguishable from *M. australis* [61] and was even treated as a synonym of the latter [4]. The diagnostic features of *M. kagayamae* include its female flowers with long styles and its leaf margins with sharp acuminate teeth [58] (Table S1); based on these characters this species may be distinctive and warrants further investigation. *Morus koordersiana* was listed by Gardner et al. [5] with a note that it might be synonymous with *M. macroura*. Specimens (Plasschaert, Sept. 1913, P (P06759968, P06759969, P06759970, P06759974; <https://science.mnhn.fr/institution/mnhn/collection/p/list>, accessed on 1 September 2022)) initially identified as *M. macroura* by S. H. Koorders and T. Valetton [8] later became the basis for J.F. Leroy's new species, *M. koordersiana*, which he separated with some "hesitation" based on its longer syncarp, weaker indumentum, and more orbicular leaves with a more consistent margin [8]. We examined images of the specimens and found them consistent with the expected variation found in the widespread

M. macroura; we therefore provisionally consider *M. koordersiana* as a synonym of *M. macroura*.

Another controversial species, *Morus indica*, has been considered a variety of *M. alba* [7,62]. This variety (*M. alba* var. *indica*) was treated as a synonym of *M. australis* by Zhou and Gilbert [1] and Nepal and Purintun [4]. *Morus indica* can be distinguished by the fine indumentum on the abaxial leaf surface. We note, however, that the putative example of *M. indica* sequenced by Gardner et al. [5], which was sister to the rest of the *M. alba* clade and subsequently re-determined as *M. cf. alba*, shows some leaf characters that might be considered intermediate between the two species. It therefore warrants additional investigation.

4.2. Phylogenetic Relationships

Until recently, *Morus s.l.* was non-monophyletic [4,13] with the inclusion of *M. mesozygia* and *M. insignis*. A monophyletic *Morus s.s.* was recognized by Gardner et al. [5] by excluding *M. mesozygia* (= *A. mesozygia*) and *M. insignis* (= *P. insignis*), which is supported by our phylogenetic results. Consistent with previous molecular phylogenetic studies [5,63], our study also supported *Morus* as a member of tribe Moreae, and sister to *Trophis*.

The molecular phylogenetic study of Nepal and Ferguson [13] resolved subg. *Morus* into an Asian clade and a North American clade, which is largely supported in the current study. However, the Asian *M. notabilis* sampled in Nepal and Ferguson [13] was incorrectly identified [64]. The current study and Gardner et al. [5] sampled *M. notabilis*, and both found support for it as sister of the remaining species of *Morus*. *Morus notabilis* is distributed in Yunnan and Sichuan provinces of China and is distinguished from other *Morus* species by its orbicular leaves, female flowers with long styles, and long syncarps (Figure 1; Table S1). This species has 14 chromosomes [65,66], but haplotype of a certain individual has six chromosomes [67] (due to mitotic chromosomes 5 and 7 fused to form meiotic chromosome 5, detailed in Xuan et al. [67]), compared to other *Morus* species with 28 (e.g., *M. alba* [68], *M. rubra* [69]), 84 (e.g., *M. serrata* [70]), or even 308 (e.g., *M. nigra* [71]) chromosomes (Table S1). Xuan et al. [67] inferred that chromosomal fission/fusion events resulted in the different basic chromosome numbers between *M. notabilis* and *M. alba*. We speculate the chromosomal fission/fusion events triggered the divergence between the ancestor of *M. notabilis* and the ancestor of the other *Morus* species.

The American clade has been supported in previous studies (e.g., Nepal and Purintun [4]; Gardner et al. [5]; Nepal and Ferguson [13]) and comprises two species: *M. rubra*, which is distributed in the temperate region from Southeast Canada to Central and eastern U.S.A., and *M. celtidifolia*, which is found in the tropical region from Mexico to Bolivia. *Morus rubra* is distinguished from *M. celtidifolia* by its larger, abaxially pubescent leaf and its more compactly arranged fruiting perianths, while *M. celtidifolia* has leaves that are abaxially pubescent only along the veins and fruiting perianths arranged loosely in the syncarps.

All previous and our current molecular phylogenetic studies have included some species of the Asian clade. Phylogenetic studies using ITS and *trnL-trnF* [4,13] have poorly resolved the interspecific relationships among seven sampled species of the Asian clade. Our study and Gardner et al. [5] using large numbers of nuclear loci largely resolved consistent topologies despite some nodes obtaining only moderate support; however, only seven and five species were sampled in these two studies. Furthermore, the phylogenetic relationships among *M. cathayana*, *M. mongolica*, and a lineage comprising *M. alba* and *M. australis* remained unresolved in the current study, with two different topologies inferred in the concatenated ML tree and the ASTRAL tree.

Our analyses suggested that both reticulation events and to some extent ILS may have been involved in the diversification of the two Asian clades. Hybridization between *Morus* species has been frequently reported (e.g., Das and Krishnaaswami [10]; Burgess et al. [11]; Muhonja et al. [12]). Our phylogenetic network analysis reveals three reticulation events in *Morus*. In particular, the possible hybrid origin of *M. cathayana* may be responsible for

the difficulty in resolving the phylogenetic position of this species. Furthermore, extensive ILS in the Asian clade may be another main reason for the poorly resolved relationships of this clade. All putative species should be included to fully resolve the phylogenetic relationships of this clade and explore the hybridization events within *Morus*.

Life history and morphological characters including breeding system, syncarp length, and style length have been commonly used to identify *Morus* species (e.g., Zhou and Gilbert [1]; Koidzumi [2]; Chang et al. [3]). We reconstructed the ancestral states of these three morphological characters, and the results indicated that the common ancestor of *Morus* was dioecious (Figure 7A), had short syncarps (Figure 7B), and had short or long styles (Figure 7C). The transition from dioecy to monoecy and dioecy + monoecy occurred one time, respectively. The transitions from short syncarp to long syncarp occurred three times. The two sections (sect. *Macromorus* and sect. *Dolichostylae*) established by Koidzumi [2] based on the length of styles are non-monophyletic. None of these characters is synapomorphic for either the American clade or the Asian Clade.

4.3. Biogeographic History

Our biogeographic analysis indicated that *Morus* had split from its sister group, *Trophis*, at the Oligocene-Eocene boundary in one of three regions of the Sino-Himalayan region, the Sino-Japanese region, and the Americas (Figure 6). The crown ancestor of *Morus* was inferred to be in the Sino-Himalayan region or the Americas, which then diversified into three distinct lineages with range expansion further into the Sino-Japanese region and Southeast Asia since the middle Miocene (Figure 6).

The Asian-North American disjunction of *Morus* could be the remnant of once widely developed temperate forests during the Tertiary (e.g., Xiang et al. [14]; Wen [15]; Boufford and Spongberg [18]). In the early Tertiary, a “boreotropical” flora was suggested to be widespread in the Northern Hemisphere [72,73]. The “boreotropical” flora could exchange floristic elements between Asia and North America via the Bering Land Bridge (BLB) and between Europe and North America via the North Atlantic Land Bridge (NALB) beginning in the late Eocene [74]. After the mid-Tertiary, the “boreotropical” flora gradually developed into a “mixed mesophytic forest” [18,75]. Many taxa in the forest became extinct in western North America and western Europe during the late Tertiary and Quaternary [14,15,76]. *Morus* might have originated as part of the “boreotropical” flora and diversified during the rise in the “mixed mesophytic forest” and formed a wide distribution in the Northern Hemisphere. The extensive local extinction events (Figure 6) that took place since the early Miocene—including those occurring following the divergence of *M. notabilis* and the rest of *Morus*, the split of the Asian and American clades, as well as the separation of eastern Asia and western Asia—may have resulted from the fragmentation of the “mixed mesophytic forest”. Multiple *Morus* fossil fruits and leaves from the late Eocene to the late Neogene (Table S5) have been found in high latitude regions of Eurasia, indicating a great reduction in the distribution of *Morus* species toward the present.

The Sino-Japanese Floristic Region has received wide attention due to its extremely high temperate species diversity [75,77,78]. It was a significant glacial refuge for temperate plants during the Quaternary Ice Age [78]. The extensive climate and physiographical heterogeneity, combined with the lack of major Quaternary glaciations, may lead to the exceptional species diversity in this region [77,78]. It is the center of diversity for *Morus*, and hosts nine of the 16 recognized species.

Morus experienced two southward dispersals to Southeast Asia from the Sino-Himalayan and Sino-Japanese regions during the late Miocene to the middle Pliocene. The uplift of Thai-Malay peninsula, Sumatra, and Java along the Barisan Mountains supplied a potential channel for the two dispersals [79,80]. Multiple plant taxa show southward migrations during this period (e.g., Jin et al. [16]). Given that *Morus* species have colorful and juicy syncarps that are frequently eaten by birds [81,82], long-distance dispersals via birds may have facilitated these two migrations.

5. Conclusions

In this study, we used new and previous data to build phylogenetic trees, providing a basis for studying the biogeographic history of this genus. The phylogenetic relationships within *Morus* were generally well supported; however, some nodes of the Asian clade only had moderate support. We inferred that both reticulation events and ILS may have contributed to the unresolved phylogenetic position of *M. cathayana*. We traced the origin of the *Morus* crown back to the early Miocene period, and the disjunct distribution of this genus was inferred to represent remnants of the once widespread Tertiary temperate forests. This finding corresponds with the rich fossil records of *Morus* in the Northern Hemisphere since the late Eocene. Moreover, several dispersal events likely led to the establishment of *Morus* in the Sino-Japanese region and Southeast Asia.

Supplementary Materials: The following supporting information can be downloaded at: <https://www.mdpi.com/article/10.3390/agronomy13082021/s1>, Figure S1. Images of *Morus* specimens from herbaria. Collector and collection number are listed in brackets. A, *M. alba* (A. C. Sanders, 13809); B, *M. australis* (M. Ono and S. Kobayashi, 123507); C, *M. cathayana* (Gaoligong Shan Biodiversity Survey, 19616); D, *M. cathayana* (Nie Min-Xiang, 92144); E, *M. cathayana* (E. M. Wilson, 10); F, *M. celtidifolia* (Juan Calzada, 20974); G, *M. celtidifolia* (Sandoval and Gutierrez, 637); H, *M. kagayamae* Koidz. (AA20187-A); I, *M. macroura* (Gardner, 28); J, *M. microphylla* (Fishbein et al., 1058); K, *M. mongolica* (Liu Xin-Yuan, 5257); L, *M. nigra* (Gardner, 29); M, *M. notabilis* (Gaoligong Shan Biodiversity Survey, 29353); N, *M. rubra* (Steven R. Hill, 36694); O, *M. serrata* (Koelz, 4788); P, *M. wittorum* (Zhang Wei). Figure S2. The ASTRAL tree (left) and concatenated ML tree (right) of *Morus* based on the C430 matrix. Figure S3. Result of the polytomy test based on the simplified C157 matrix. Figure S4. The result of coalescent simulations with 1000 trees simulated under the coalescent mapped against the concatenated ML tree of the C157 dataset. The numbers near the branches indicate the number of simulated trees that are concordant (above) and discordant (below) with a given branch. The pie chart at each node indicates the proportion of simulated trees that are concordant (blue) with a given node, support a dominant alternative topology (green), and support the remaining alternative topologies (red). Table S1. Diagnostic features, number of chromosomes, and distribution of *Morus*. Table S2. Characteristics of all datasets for reconstructing the phylogeny of *Morus*. Table S3. Results of the AU tests for two sets of discordant topologies. Table S4. LnL and AIC values of biogeographic models. Table S5. Fossil record of *Morus*.

Author Contributions: C.-X.Y. and T.-S.Y. designed the paper. C.-X.Y. performed the data analysis and wrote the manuscript with the support of T.-S.Y. R.A.F. designed the HybSeq100 probes. D.E.S., G.W.S., H.R.K., Q.T., R.A.F., R.P.G., S.-Y.L., T.-S.Y. and P.S.S. collected the plant material and extracted the total DNA. D.E.S., H.R.K., R.A.F., R.P.G. and P.S.S. contributed to the sequencing. D.E.S., E.M.G., G.W.S., N.J.C.Z., P.S.S., Q.L., R.A.F., R.P.G., S.-Y.L., T.-S.Y., W.G. and Y.-H.W. revised the manuscript. All authors have read and agreed to the published version of the manuscript.

Funding: This research was supported by the National Natural Science Foundation of China, key international (regional) cooperative research project (No. 31720103903), the Strategic Priority Research Program of Chinese Academy of Sciences (No. XDB31000000), the Science and Technology Basic Resources Investigation Program of China (No. 2019FY100900), the National Natural Science Foundation of China (No. 31270274), the Yunling International High-end Experts Program of Yunnan Province, China (No. YNQR-GDWG-2017-002 and No. YNQR-GDWG-2018-012), the CAS President's International Fellowship Initiative (No. 2020PB0009), the China Postdoctoral Science Foundation (CPSF) International Postdoctoral Exchange Program, and the CAS Special Research Assistant Project. This work was also supported in part by USA Department of Energy grant DE-SC0018247.

Data Availability Statement: Raw sequence data are available at the NCBI Sequence Read Archive (BioProject: PRJNA980892). The configuration file aligned DNA sequences and trees are available on Dryad Digital Repository: <https://doi.org/10.5061/dryad.bzkh189g1>.

Acknowledgments: We are grateful to the following institutes for providing specimens or silica-dried materials: Herbarium of Kunming Institute of Botany, Chinese Academy of Sciences (KUN); the Germplasm Bank of Wild Species and Molecular Biology Experiment Center, Kunming Institute of Botany, Chinese Academy of Sciences; the herbarium of the California Academy of Sciences (CAS); the Chicago Botanic Garden (CHIC); the Field Museum (F); the Royal Botanic Gardens, Kew (K); the

Missouri Botanical Garden (MO); the Morton Arboretum (MOR); the US National Tropical Botanical Garden (PTBG); the New York Botanical Garden (NY); the Ohio State University Herbarium (OS); the Sandakan Herbarium, Forest Research Centre (SAN); and the University of Texas Herbarium (TEX). We are also grateful to Jia-Jin Wu for help with sampling; to Hua-Feng Wang, Diego F. Morales-Briones, Nelson Zamora Villalobos, Rong Zhang, Hui Liu, Si-Yun Chen, Xiao-Gang Fu, Ying-Ying Yang, and Henrique Borges Zamengo for their generous technical support and necessary assistance; to Greta Buttelmann for assistance in identifying specimens; and to the iFlora High Performance Computing Center of the Germplasm Bank of Wild Species (iFlora HPC Center of GBOWS, KIB, CAS) for computing. We appreciate the photos provided by Jie Cai of the Germplasm Bank of Wild Species, Kunming Institute of Botany, Chinese Academy of Sciences, Qin Tian (SFU) of the Southwest Forestry University, Qin-Wen Lin of the Institute of Botany, Chinese Academy of Sciences, Si-Yu Zhang of the Anhui Normal University, and Xin-Xin Zhu of Xinyang Normal University.

Conflicts of Interest: The authors declare no conflict of interest.

References

- Zhou, Z.K.; Gilbert, M.G. Moraceae. In *Flora of China*; Wu, Z.Y., Raven, P.H., Hong, D.Y., Eds.; Missouri Botanical Garden Press: St. Louis, MO, USA; Science Press: Beijing, China, 2003; Volume 5, pp. 22–26.
- Koidzumi, G. Taxonomy and phytogeography of the genus *Morus*. *Bull. Sericultural Exp. Stn.* **1917**, *3*, 1–61.
- Chang, S.S.; Wu, C.Y.; Cao, Z.Y. Moraceae. In *Flora Reipublicae Popularis Sinicae*; Chang, S.S., Wu, C.Y., Eds.; Science Press: Beijing, China, 1998; Volume 23, pp. 6–23.
- Nepal, M.P.; Purinton, J.M. Systematics of the genus *Morus* L. (Moraceae) taxonomy, phylogeny and potential responses to climate change. In *Mulberry: Genetic Improvement in Context of Climate Change*; Razdan, M.K., Thomas, D.T., Eds.; The CRC Press: Boca Raton, FL, USA, 2021; pp. 2–20.
- Gardner, E.M.; Garner, M.; Cowan, R.; Dodsworth, S.; Epiawalage, N.; Arifiani, D.; Sahromi; Baker, W.J.; Forest, F.; Maurin, O.; et al. Repeated parallel losses of inflexed stamens in Moraceae: Phylogenomics and generic revision of the tribe Moreae and the reinstatement of the tribe Olmedieae (Moraceae). *Taxon* **2021**, *70*, 946–988. [[CrossRef](#)]
- Linnaeus, C. *Morus*. *Species Plant.* **1753**, *2*, 968.
- Bureau, E. Moraceae. *Prodromus Syst. Nat. Regni Veg.* **1873**, *17*, 211–279.
- Leroy, J.F. Contribution a l'étude des Monochlamydees: Documents nouveaux sur des plantes de Madagascar, de Sumatra et de Colombie. *Bull. Mus. Hist. Nat. Paris* **1949**, *21*, 725–732.
- Hotta, T. Fundamentals of *Morus* plants classification. *Kinugasa Sanpo* **1954**, *390*, 13–21.
- Das, B.C.; Krishaaswami, S. Some observations on interspecific hybridization in mulberry. *Indian J. Seric.* **1965**, *4*, 1–4.
- Burgess, K.S.; Morgan, M.; Husband, B.C. Interspecific seed discounting and the fertility cost of hybridization in an endangered species. *New Phytol.* **2008**, *177*, 276–284. [[CrossRef](#)]
- Muhonja, L.; Yamanouchi, H.; Yang, C.C.; Kuwazaki, S.; Yokoi, K.; Kameda, T.; Sezutsu, H.; Jouraku, A. Genome-wide SNP marker discovery and phylogenetic analysis of mulberry varieties using double-digest restriction site-associated DNA sequencing. *Gene* **2020**, *726*, 144162. [[CrossRef](#)]
- Nepal, M.P.; Ferguson, C.J. Phylogenetics of *Morus* (Moraceae) inferred from ITS and *trnL-trnF* sequence data. *Syst. Bot.* **2012**, *37*, 442–450. [[CrossRef](#)]
- Xiang, Q.-Y.; Soltis, D.E.; Soltis, P.S. The Eastern Asian and Eastern and Western North American Floristic Disjunction: Congruent Phylogenetic Patterns in Seven Diverse Genera. *Mol. Phylogenet. Evol.* **1998**, *10*, 178–190. [[CrossRef](#)] [[PubMed](#)]
- Wen, J. Evolution of Eastern Asian and Eastern North American Disjunct Distributions in Flowering Plants. *Annu. Rev. Ecol. Syst.* **1999**, *30*, 421–455. [[CrossRef](#)]
- Jin, J.J.; Yang, M.Q.; Fritsch, P.W.; Velzen, R.; Li, D.Z.; Yi, T.S. Born migrators: Historical biogeography of the cosmopolitan family Cannabaceae. *J. Syst. Evol.* **2019**, *58*, 461–473. [[CrossRef](#)]
- Gaynor, M.L.; Fu, C.N.; Gao, L.M.; Lu, L.M.; Soltis, D.E.; Soltis, P.S. Biogeography and ecological niche evolution in Diapensiaceae inferred from phylogenetic analysis. *J. Syst. Evol.* **2020**, *58*, 646–662. [[CrossRef](#)]
- Boufford, D.E.; Spongberg, S.A. Eastern Asian-Eastern North American Phytogeographical Relationships—A History from the Time of Linnaeus to the Twentieth Century. *Ann. Mo. Bot. Gard.* **1983**, *70*, 423. [[CrossRef](#)]
- Williams, E.W.; Gardner, E.M.; Harris, R.; Chaveerach, A.; Pereira, J.; Zerega, N.J.C. Out of Borneo: Biogeography, phylogeny and divergence date estimates of *Artocarpus* (Moraceae). *Ann. Bot.* **2017**, *119*, 611–627. [[CrossRef](#)] [[PubMed](#)]
- Zerega, N.J.; Clement, W.L.; Datwyler, S.L.; Weiblen, G.D. Biogeography and divergence times in the mulberry family (Moraceae). *Mol. Phylogenet. Evol.* **2005**, *37*, 402–416. [[CrossRef](#)]
- Doyle, J.; Doyle, J. Genomic plant DNA preparation from fresh tissue-CTAB method. *Phytochem. Bull.* **1987**, *19*, 11–15.
- Folk, R.A.; Kates, H.R.; LaFrance, R.; Soltis, D.E.; Soltis, P.S.; Guralnick, R.P. High-throughput methods for efficiently building massive phylogenies from natural history collections. *Appl. Plant Sci.* **2021**, *9*, e11410. [[CrossRef](#)]

23. Kates, H.R.; O'Meara, B.C.; LaFrance, R.; Stull, G.W.; James, E.K.; Conde, D.; Liu, S.Y.; Tian, Q.; Yi, T.S.; Kirst, M.; et al. Two shifts in evolutionary lability underlie independent gains and losses of root-nodule symbiosis in a single clade of plants. *bioRxiv* **2022**. [[CrossRef](#)]
24. Fu, X.G.; Liu, S.Y.; van Velzen, R.; Stull, G.W.; Tian, Q.; Li, Y.X.; Folk, R.A.; Guralnick, R.P.; Kates, H.R.; Jin, J.J.; et al. Phylogenomic analysis of the hemp family (Cannabaceae) reveals deep cyto-nuclear discordance and provides new insights into generic relationships. *J. Syst. Evol.* **2022**. [[CrossRef](#)]
25. Liu, S.Y.; Yang, Y.Y.; Tian, Q.; Yang, Z.Y.; Li, S.F.; Valdes, P.J.; Farnsworth, A.; Kates, H.R.; Siniscalchi, C.M.; Guralnick, R.P.; et al. Phylogenomic analyses reveal widespread gene flow during the early radiation of oaks and relatives (Fagaceae: Quercoideae). *bioRxiv* **2023**. [[CrossRef](#)]
26. Bolger, A.M.; Lohse, M.; Usadel, B. Trimmomatic: A flexible trimmer for Illumina sequence data. *Bioinformatics* **2014**, *30*, 2114–2120. [[CrossRef](#)] [[PubMed](#)]
27. Johnson, M.G.; Gardner, E.M.; Liu, Y.; Medina, R.; Goffinet, B.; Shaw, A.J.; Zerega, N.J.C.; Wickett, N.J. HybPiper: Extracting coding sequence and introns for phylogenetics from high-throughput sequencing reads using target enrichment. *Appl. Plant Sci.* **2016**, *4*, 1600016. [[CrossRef](#)] [[PubMed](#)]
28. Katoh, K.; Standley, D.M. MAFFT Multiple Sequence Alignment Software Version 7: Improvements in Performance and Usability. *Mol. Biol. Evol.* **2013**, *30*, 772–780. [[CrossRef](#)]
29. Baker, W.J.; Bailey, P.; Barber, V.; Barker, A.; Bellot, S.; Bishop, D.; Botigué, L.R.; Brewer, G.; Carruthers, T.; Clarkson, J.J.; et al. A Comprehensive Phylogenomic Platform for Exploring the Angiosperm Tree of Life. *Syst. Biol.* **2022**, *71*, 301–319. [[CrossRef](#)]
30. Huerta-Cepas, J.; Serra, F.; Bork, P. ETE 3: Reconstruction, Analysis, and Visualization of Phylogenomic Data. *Mol. Biol. Evol.* **2016**, *33*, 1635–1638. [[CrossRef](#)]
31. Capella-Gutierrez, S.; Silla-Martinez, J.M.; Gabaldon, T. trimAl: A tool for automated alignment trimming in large-scale phylogenetic analyses. *Bioinformatics* **2009**, *25*, 1972–1973. [[CrossRef](#)]
32. Zerega, N.J.; Gardner, E.M. Delimitation of the new tribe Parartocarpeae (Moraceae) is supported by a 333-gene phylogeny and resolves tribal level *Moraceae* taxonomy. *Phytotaxa* **2019**, *388*, 253–265. [[CrossRef](#)]
33. Johnson, M.G.; Pokorný, L.; Dodsworth, S.; Botigué, L.R.; Cowan, R.S.; Devault, A.; Eiserhardt, W.L.; Epitawalage, N.; Forest, F.; Kim, J.T.; et al. A Universal Probe Set for Targeted Sequencing of 353 Nuclear Genes from Any Flowering Plant Designed Using k-Medoids Clustering. *Syst. Biol.* **2019**, *68*, 594–606. [[CrossRef](#)]
34. Stamatakis, A. RAxML version 8: A tool for phylogenetic analysis and post-analysis of large phylogenies. *Bioinformatics* **2014**, *30*, 1312–1313. [[CrossRef](#)] [[PubMed](#)]
35. Mirarab, S.; Reaz, R.; Bayzid, M.S.; Zimmermann, T.; Swenson, M.S.; Warnow, T. ASTRAL: Genome-scale coalescent-based species tree estimation. *Bioinformatics* **2014**, *30*, i541–i548. [[CrossRef](#)] [[PubMed](#)]
36. Shimodaira, H. An Approximately Unbiased Test of Phylogenetic Tree Selection. *Syst. Biol.* **2002**, *51*, 492–508. [[CrossRef](#)] [[PubMed](#)]
37. Shimodaira, H.; Hasegawa, M. CONSEL: For assessing the confidence of phylogenetic tree selection. *Bioinformatics* **2001**, *17*, 1246–1247. [[CrossRef](#)] [[PubMed](#)]
38. Sayyari, E.; Mirarab, S. Testing for Polytomies in Phylogenetic Species Trees Using Quartet Frequencies. *Genes* **2018**, *9*, 132. [[CrossRef](#)]
39. García, N.; Folk, R.A.; Meerow, A.W.; Chamala, S.; Gitzendanner, M.A.; de Oliveira, R.S.; Soltis, D.E.; Soltis, P.S. Deep reticulation and incomplete lineage sorting obscure the diploid phylogeny of rain-lilies and allies (Amaryllidaceae tribe Hippeastreae). *Mol. Phylogenet. Evol.* **2017**, *111*, 231–247. [[CrossRef](#)]
40. Wang, H.X.; Morales-Briones, D.F.; Moore, M.J.; Wen, J.; Wang, H.F. A phylogenomic perspective on gene tree conflict and character evolution in Caprifoliaceae using target enrichment data, with Zabelioideae recognized as a new subfamily. *J. Syst. Evol.* **2021**, *59*, 897–914. [[CrossRef](#)]
41. Mirarab, S.; Bayzid, S.; Boussau, B.; Warnow, T. Statistical binning enables an accurate coalescent-based estimation of the avian tree. *Science* **2014**, *346*, 1250463. [[CrossRef](#)]
42. Smith, S.A.; Moore, M.J.; Brown, J.W.; Yang, Y. Analysis of phylogenomic datasets reveals conflict, concordance, and gene duplications with examples from animals and plants. *BMC Ecol. Evol.* **2015**, *15*, 1–15.
43. Than, C.; Ruths, D.; Nakhleh, L. PhyloNet: A software package for analyzing and reconstructing reticulate evolutionary relationships. *BMC Bioinform.* **2008**, *9*, 322. [[CrossRef](#)]
44. Yu, Y.; Degnan, J.H.; Nakhleh, L. The Probability of a Gene Tree Topology within a Phylogenetic Network with Applications to Hybridization Detection. *PLoS Genet.* **2012**, *8*, e1002660. [[CrossRef](#)]
45. Zhang, Q.; Onstein, R.E.; Little, S.A.; Sauquet, H. Estimating divergence times and ancestral breeding systems in *Ficus* and *Moraceae*. *Ann. Bot.* **2019**, *123*, 191–204. [[CrossRef](#)] [[PubMed](#)]
46. Mehrotra, R.; Prakash, U.; Bande, M. Fossil woods of *Lophopetalum* and *Artocarpus* from the Deccan Intertrappean beds of Mandla District, Madhya Pradesh, India. *J. Palaeosci.* **1984**, *32*, 310–320. [[CrossRef](#)]
47. Chandler, M.E.J. *The Lower Tertiary Floras of Southern England: Flora of the Pipe-Clay 29 Series of Dorset (Lower Bagshot)*; British Museum: London, UK, 1962; pp. 1–169.

48. Collinson, M.E. The fossil history of the Moraceae, Urticaceae (including Cecropiaceae), and Cannabaceae. In *Evolution, Systematics, and Fossil History of the Hamamelidae. Systematics Association Special*; Crane, P.R., Blackmore, S., Eds.; Clarendon Press: Oxford, UK, 1989; Volume 40B, pp. 319–339.
49. Smith, S.A.; O’Meara, B.C. TreePL: Divergence time estimation using penalized likelihood for large phylogenies. *Bioinformatics* **2012**, *28*, 2689–2690. [[CrossRef](#)]
50. Maurin, K.J.L. An empirical guide for producing a dated phylogeny with treePL in a maximum likelihood framework. *arXiv* **2020**, arXiv:2008.07054.
51. Bouckaert, R.; Heled, J.; Kühnert, D.; Vaughan, T.; Wu, C.-H.; Xie, D.; Suchard, M.A.; Rambaut, A.; Drummond, A.J. BEAST 2: A Software Platform for Bayesian Evolutionary Analysis. *PLoS Comput. Biol.* **2014**, *10*, e1003537. [[CrossRef](#)]
52. Wunderlin, R.P. Moraceae. In *Flora of North America North of Mexico*; Flora of North America Editorial Committee, Ed.; Oxford University Press: New York, NY, USA, 1997; Volume 3, pp. 390–392.
53. Wu, Z.Y.; Wu, S.G. A Proposal for a new floristic kingdom (realm)—The E. Asiatic Kingdom, its delineation and characteristics. In *Floristic Characteristics and Diversity of East Asian Plants*; Zhang, A.L., Wu, S.G., Eds.; China Higher Education: Beijing, China, 1996; pp. 3–42.
54. Wu, Z.Y.; Sun, H.; Zhou, Z.K. *Floristics of Seed Plants from China*; Science Press: Beijing, China, 2005; pp. 71–105.
55. Matzke, N.J. BioGeoBEARS: BioGeography with Bayesian (and likelihood) evolutionary analysis with R scripts. Version 1.1.1. *GitHub* **2018**. [[CrossRef](#)]
56. Berg, C.C. Moreae, Artocarpeae, and Dorstenia (Moraceae), with introductions to the family and Ficus and with additions and corrections to Flora Neotropica Monograph 7. *Flora Neotrop.* **2001**, *83*, 1–346.
57. Revell, L.J. phytools: An R package for phylogenetic comparative biology (and other things). *Methods Ecol. Evol.* **2011**, *3*, 217–223. [[CrossRef](#)]
58. Iwatsuki, K.; Boufford, D.E.; Ohba, H. *Flora of Japan*; Kodansha Ltd.: Tokyo, Japan, 2006; Volume IIa, pp. 74–76.
59. Chang, S.S. New Taxa of Moraceae from China and Vietnam. *Acta Phytotaxon. Sin.* **1984**, *22*, 64–76.
60. Cao, Z.Y. New taxa of *Morus* (Moraceae) from China. *J. Syst. Evol.* **1991**, *29*, 264–267.
61. Yulianti, W.; Kato, S.; Sugita, N.; Kokubugata, G.; Kato, H.; Murakami, N. Microsatellite Markers Reveal Genetic Differentiation of an Invasive Mulberry, *Morus australis* Poir. (Moraceae), among the Island Groups in Japan and its Introduction to the Ogasawara Islands. *Acta Phytotaxon. Geobot.* **2022**, *73*, 1–18.
62. Rao, C.K.; Jarvis, C.E. Lectotypification, taxonomy and nomenclature of *Morus alba*, *M. tatarica* and *M. indica* (Moraceae). *Taxon* **1986**, *35*, 705–708. [[CrossRef](#)]
63. Clement, W.L.; Weiblen, G.D. Morphological Evolution in the Mulberry Family (Moraceae). *Syst. Bot.* **2009**, *34*, 530–552. [[CrossRef](#)]
64. Zeng, Q.; Chen, H.; Zhang, C.; Han, M.; Li, T.; Qi, X.; Xiang, Z.; He, N. Definition of Eight Mulberry Species in the Genus *Morus* by Internal Transcribed Spacer-Based Phylogeny. *PLoS ONE* **2015**, *10*, e0135411. [[CrossRef](#)]
65. Yu, M.D.; Xiang, Z.H.; Feng, L.C.; Ke, Y.F.; Zhang, X.Y.; Jing, C.J. The discovery and study on a natural haploid *Morus notabilis* Schneid. *Acta Sericologica Sin.* **1996**, *22*, 67–71.
66. He, N.J.; Zhang, C.; Qi, X.W.; Zhao, S.C.; Tao, Y.; Yang, G.J.; Lee, T.-H.; Wang, X.Y.; Cai, Q.L.; Li, D.; et al. Draft genome sequence of the mulberry tree *Morus notabilis*. *Nat. Commun.* **2013**, *4*, 2445. [[CrossRef](#)]
67. Xuan, Y.H.; Ma, B.; Li, D.; Tian, Y.; Zeng, Q.W.; He, N.J. Chromosome restructuring and number change during the evolution of *Morus notabilis* and *Morus alba*. *Hortic. Res.* **2022**, *9*, uhab030. [[CrossRef](#)]
68. Jiao, F.; Luo, R.; Dai, X.; Liu, H.; Yu, G.; Han, S.; Lu, X.; Su, C.; Chen, Q.; Song, Q.; et al. Chromosome-Level Reference Genome and Population Genomic Analysis Provide Insights into the Evolution and Improvement of Domesticated Mulberry (*Morus alba*). *Mol. Plant* **2020**, *13*, 1001–1012. [[CrossRef](#)]
69. Letz, R.; Uhríková, A.; Májovský, J. Chromosomes numbers of several interesting taxa of the flora of Slovakia. *Biologia* **1999**, *54*, 43–49.
70. Dandia, B.S.B.; Rajan, M.V. Microsporogenesis in hexaploid *Morus serrata* Roxb. *Cytologia* **1989**, *54*, 747–751.
71. Basavaiah; Dandia, S.B.; Dhar, A.; Sengupta, K. Meiosis in natural decosaploid(22x) *Morus nigra* L. *Cytologia* **1990**, *55*, 505–509. [[CrossRef](#)]
72. Wolfe, J.A. Neogene floristic and vegetational history of the Pacific Northwest. *Madrono* **1969**, *20*, 83–110.
73. Wolfe, J.A. Some Aspects of Plant Geography of the Northern Hemisphere During the Late Cretaceous and Tertiary. *Ann. Mo. Bot. Gard.* **1975**, *62*, 264. [[CrossRef](#)]
74. Aradhya, M.K.; Potter, D.; Gao, F.Y.; Simon, C.J. Molecular phylogeny of *Juglans* (Juglandaceae): A biogeographic perspective. *Tree Genet. Genomes* **2007**, *3*, 363–378. [[CrossRef](#)]
75. Tiffney, B.H. Perspectives on the origin of the floristic similarity between Eastern Asia and Eastern North America. *J. Arnold Arbor.* **1985**, *66*, 73–94. [[CrossRef](#)]
76. Graham, A. History of the vegetation: Cretaceous (Maastrichtian)—Tertiary. In *Flora of North America North of Mexico*; Flora of North America Editorial Committee, Ed.; Oxford University Press: New York, NY, USA, 1993; Volume 1, pp. 57–70.
77. Qian, H.; Ricklefs, R.E. Large-scale processes and the Asian bias in species diversity of temperate plants. *Nature* **2000**, *407*, 180–182. [[CrossRef](#)]

78. Qiu, Y.X.; Fu, C.X.; Comes, H.P. Plant molecular phylogeography in China and adjacent regions: Tracing the genetic imprints of Quaternary climate and environmental change in the world's most diverse temperate flora. *Mol. Phylogenet. Evol.* **2011**, *59*, 225–244. [[CrossRef](#)]
79. Barber, A.J.; Crow, M.J.; Milsom, J.S. *Sumatra: Geology, Resources and Tectonic Evolution*; Geological Society: London, UK, 2005; p. 96.
80. Hall, R. Southeast Asia's changing palaeogeography. *Blumea-Biodivers. Evol. Biogeogr. Plants* **2009**, *54*, 148–161. [[CrossRef](#)]
81. Barnea, A.; Yom-Tov, Y.; Friedman, J. Effect of frugivorous birds on seed dispersal and germination. *Acta Oecologica* **1992**, *13*, 209–219.
82. Corlett, R.T. Interactions between birds, fruit bats and exotic plants in urban Hong Kong, South China. *Urban Ecosyst.* **2005**, *8*, 275–283. [[CrossRef](#)]

Disclaimer/Publisher's Note: The statements, opinions and data contained in all publications are solely those of the individual author(s) and contributor(s) and not of MDPI and/or the editor(s). MDPI and/or the editor(s) disclaim responsibility for any injury to people or property resulting from any ideas, methods, instructions or products referred to in the content.